Epilepsy Research 61 (2004) 89–104

Epilepsy Research

www.elsevier.com/locate/epilepsyres

Pre-ictal synchronicity in limbic networks of mesial temporal lobe epilepsy

F. Bartolomei[a,*], F. Wendling[b], J. Régis[a], M. Gavaret[a], M. Guye[a], P. Chauvel[a]

[a] *Service de Neurophysiologie Clinique, INSERM EMI 9926, CHU TIMONE et Université de la Méditerranée, 13385 Marseille Cedex 5, France*

[b] *Laboratoire Traitement du Signal et de L'Image, INSERM U642, Université de Rennes 1, Campus de Beaulieu, 35042 Rennes Cedex, France*

Received 18 April 2004; received in revised form 14 June 2004; accepted 21 June 2004

Abstract

Purpose: We recorded with intracerebral electrodes the onset of limbic seizures in patients with mesial temporal lobe epilepsy (MTLE) to identify the dynamic interactions between the hippocampus (HIP), amygdala (AMY) and entorhinal cortex (EC). *Methods:* Interactions were quantified by analyzing the interdependencies between stereo-electroencephalographic (SEEG) signals using a nonlinear cross-correlation method. Seizures from 12 patients were analyzed by identifying three periods of interest: (i) the rapid discharge that occurs at seizure onset ("during rapid discharge", DRD period); (ii) the time interval that precedes this rapid discharge ("before rapid discharge", BRD period); and the time that follows the rapid discharge ("after rapid discharge", ARD period). The transition from interictal to ictal discharge was classified into: (i) "type 1 transition" in which the emergence of pre-ictal spiking was followed by a rapid discharge; and (ii) "type 2 transition" that was associated with rapid discharge onset without prior spiking. *Results:* In both types of transition the BRD period was characterized by significant cross-correlation values indicating strong interactions among mesial temporal structures as compared to those seen during background activity. Interactions between HIP and EC were predominant in 10 of 12 patients (83%). Interactions between EC and AMY were observed in 6 of 12 cases (50%) and between AMY and HIP in 7 of 12 cases (58%). Analysis of coupling directionality indicated that most of the couplings were driven either by HIP (six patients) or by the EC (four patients). The DRD period was characterized by a significant decrease of cross-correlation values. In addition, type 1 transition was characterized by interactions that uniformly involved the three structures, while type 2 transition was associated with interactions between EC and HIP. Finally, analysis of coupling direction demonstrated that the HIP was always the leader in type 1 transition whereas in type 2 the EC was most often the leading structure.

* Corresponding author. Present address: Service de Neurophysiologie Clinique, CHU Timone-264 Rue st Pierre 13005-Marseille, France. Tel.: +33 491 385833; fax: +33 491 385826.

E-mail address: fbartolo@medecine.univ-mrs.fr (F. Bartolomei).

0920-1211/$ – see front matter
doi:10.1016/j.eplepsyres.2004.06.006

Conclusions: This study demonstrates that pre-ictal synchronization between mesial structures is the initial event for seizures starting in the mesial temporal region.

Keywords: Temporal lobe; Epilepsy; Neural networks; Signal processing; Entorhinal cortex

1. Introduction

Seizures in patients with mesial temporal lobe epilepsy (MTLE) are the most common form of partial epileptic seizures (Williamson et al., 1998). Since they are often resistant to antiepileptic drug treatment, detailed study of the functional organization of the epileptogenic zone in MTLE patients may provide important indications for therapeutic approaches such as selective surgery, selective radio surgery or depth stimulations. Depth-EEG recordings performed with intracerebral electrodes during pre-surgical evaluation have shown that seizures in MTLE patients are generated within the mesial part of the temporal lobe (Bancaud, 1981; Engel et al., 1989; Spencer et al., 1992). However, the precise functional organization of the epileptogenic zone is still a matter of debate (Bartolomei et al., 2001; Bertram et al., 1998).

According to the "focal" model, a single pathological region is responsible for seizure generation. Accordingly, in the past, most studies have focussed on the role of hippocampal alterations in MTLE and some of these investigations have established a link between the presence of hippocampal atrophy and the area of seizure onset (King et al., 1997). In contrast, the "network" model holds that limbic seizures may result from a more extensive alteration of limbic networks within the temporal lobe (Bartolomei et al., 2001; Bertram et al., 1998). Recent findings support this second view. Besides hippocampal atrophy, recent studies have demonstrated a reduction in the volume of other limbic regions, such as the entorhinal cortex in MTLE patients (Bernasconi et al., 1999, 2000; Jutila et al., 2001) (Du et al., 1993). Moreover, experimental studies indicate that seizure onset in MTLE models involves several limbic regions (Avoli et al., 2002; Bertram et al., 1998).

Depth electrode studies in MTLE patients have also revealed that epileptic discharges may be recorded from several limbic regions, including the hippocampus and the entorhinal cortex (Bartolomei et al., 2001; Velasco et al., 2000a). However, in this situation, the relative contribution of the different mesial structures (amygdala, rhinal cortices and hippocampus) remains poorly understood in humans, even though studies in human (Spencer and Spencer, 1994) or animal models (Barbarosie et al., 2000; Lothman et al., 1991) have suggested that the abnormal interaction between entorhinal cortex and hippocampal formations may be responsible for seizures.

In this paper, we analyzed the dynamics of interactions between three limbic areas (i.e., amygdala, entorhinal cortex and hippocampus), which were recorded with depth electrodes, during seizures in MTLE patients. These interactions were quantified by estimating the interdependencies between EEG signals. Specifically, a signal processing method based on nonlinear regression analysis (Meeren et al., 2002; Pijn, 1990; Wendling et al., 2001) was applied to depth-EEG time series in order to characterize the evolution of their cross-correlation. Based on the analysis of interactions between regions at the onset of seizures recorded intracerebrally, our results support the "epileptogenic network" hypothesis, namely that synchronized oscillations among spatially distributed limbic structures represent the substratum of the epileptogenic zone leveling this epileptic disorder .

2. Methods

2.1. Patient selection and SEEG recording

Twelve patients undergoing pre-surgical evaluation of drug-resistant MTLE were selected. All patients had a comprehensive evaluation including detailed history and neurological examination, neuropsychological testing, routine magnetic resonance imaging (MRI), surface electroencephalography (EEG) and stereo-electroencephalography (SEEG, depth electrodes). The latter was performed during long-term video-EEG monitoring. SEEG was carried out as part of our

patient's normal clinical care, and they gave informed consent in the usual way. Patients were informed that their data might be used for research purposes.

Patients were selected for the present study if they satisfied the following criteria: (i) seizures involved the mesial temporal regions at the onset; (ii) MRI was normal or suggestive of hippocampal sclerosis (HS) (hippocampal atrophy and increased T2 signal); (iii) electrodes were placed in the entorhinal cortex, the hippocampus and the amygdala in addition to other parts of the temporal lobe (temporal pole, insular cortex, first temporal gyrus).

SEEG recordings were performed using intracerebral multiple contact electrodes (10–15 contacts, length: 2 mm, diameter: 0.8 mm, 1.5 mm apart) placed intracranially according to Talairach's stereotactic method (Musolino et al., 1990; Talairach et al., 1974). The positioning of electrodes was established in each patient based upon available non-invasive information and hypotheses about the localization of the epileptogenic zone. The implantation accuracy was peroperatively controlled by telemetric X-ray imaging. A post-operative computerized tomography (CT) scan without contrast was then used to verify the absence of bleeding and the precise location of each recording lead. Intracerebral electrodes were then removed and an MRI was performed, permitting visualization of the trajectory of each electrode. Finally, CT scan/MRI data fusion was performed to anatomically locate each contact along the electrode trajectory.

Several distinct functional regions of the temporal lobe can be explored via an orthogonal implantation of depth electrodes (Fig. 1). All the patients had electrodes that spatially sampled mesial/limbic regions (amygdala, entorhinal cortex and hippocampus) and lateral/neocortical regions of the middle temporal gyrus. The EC is the rostral part of the parahippocampal cortex extending from the limen insulae (anteriorly) to the hippocampal fissure (posteriorly) and from the subiculum (medially) to the fundus of the collateral fissure (laterally) (Insausti et al., 1995). EC was sampled with an electrode passing through the anterior temporo-basal region of the temporal lobe. This electrode recorded the middle temporal gyrus, lateral and mesial walls of the occipito-temporal and collateral fissures, and then ended in the entorhinal cortex (Fig. 1a and b).

Signals were recorded on a 128-channel Deltamed^{TM} system. They were sampled at 256 Hz and recorded on a hard disk (16 bits/sample) using no digital filter. The only filter present in the acquisition procedure was a hardware analog high-pass filter (cut-off frequency equal to 0.16 Hz) used to remove very slow variations that sometimes contaminate the baseline. Table 1 provides clinical information about the patients selected for our study.

2.2. SEEG signal analysis

2.2.1. Definition of periods of interest

Signals recorded in each patient from the hippocampus (HIP), the amygdala (AMY) and the entorhinal cortex (EC) during the transition from interictal to ictal activity were first visually analyzed. From visual inspection, a recording reflecting the most typical seizure pattern was selected for each patient. Then, for every signal of the 12 selected recordings shown in Fig. 2, the rapid discharge that occurs at seizure onset was delimited by visual inspection. In most cases, a time–frequency representation of signals (spectrogram computed from short-term fast Fourier transform) was used to accurately determine the beginning and the end of the rapid activity, as illustrated in Fig. 3. A first period of interest corresponding to the rapid discharge present on each of the three channels was then defined. This period is referred to as the DRD period ("during rapid discharge"). From the delimitation in time of the DRD period, two other periods, respectively denoted by "BRD" ("before rapid discharge") and "ARD" ("after rapid discharge") were defined (Fig. 4). The cross-correlation estimation was carried out during the whole duration of period DRD. For both BRD and ARD periods, we arbitrary chose duration of 10 s for analysis. A fourth period of background activity (BKG, duration= 10 s) was also analyzed in each patient. BKG periods were spaced at least 1 min apart from the ictal discharge and were used as reference periods in the analysis of: (i) spectral features of the SEEG signals and (ii) correlations between these signals averaged over periods of interest.

2.2.2. Spectral analysis of BKG and DRD periods

In each patient, and for each signal recorded from HIP, AMY and EC power spectral densities were computed on signals recorded over the BKG and DRD periods in order to characterize and to compare the distribution of their energy as a function of frequency

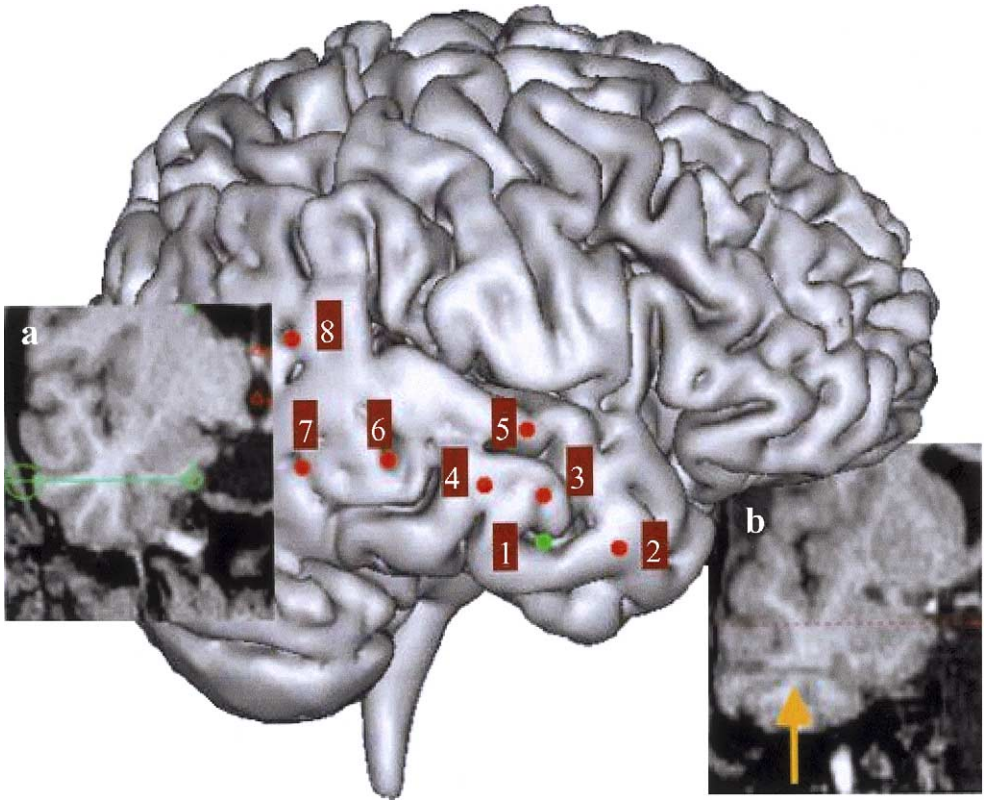

Fig. 1. Example of depth electrodes implantation for SEEG in temporal lobe epilepsy. Lateral view of all depth electrodes (patient GAR) superimposed on a 3D image. (a) and (b): coronal view of a pre-operative plan (a) and post-implantation (b) MRI of depth electrode route superimposed on a T1 MRI image. The selected slice shows the position of the electrode #1 (in green) reaching the collateral sulcus region at the end (in b, the arrow indicates the route of this electrode). Electrode #1 records the electrophysiological activity (EA) within the entorhinal cortex (internal contacts) and the anterior part of the inferior temporal gyrus (external contacts); electrode #2 records EA within the temporal pole (internal and external contacts), electrode #3 records the EA in the amygdala (internal contacts) and within the anterior part of the middle temporal gyrus (external contacts); electrode #4 records the EA within the hippocampal head (internal contacts) and the middle part of the middle temporal gyrus (external contacts), electrode #5 records EA within the anterior part of the insula (internal contacts) and the anterior part of the superior temporal gyrus (external contact); electrode #6 records EA within the hippocampal tail (internal contact) and the posterior part of the middle temporal gyrus (external contacts); electrode #7 records EA within the occipito-temporal junction and electrode #8 records EA within the isthmus of the cingulate gyrus (internal contacts) and the supra-marginalis gyrus (external contact).

(Fig. 4b). Power spectral densities were estimated by averaging power spectra computed from Fast Fourier Transform (FFT) of the time series. FFT's were performed on blocks of 256 samples (1 s) with an overlapping of 50%.

2.2.3. Estimation of average correlations over periods of interest

Correlation between signals (or cross-correlation) recorded from HIP, AMY and EC was estimated as a function of time by using nonlinear regression analysis. (Lopes da Silva et al., 1989; Pijn, 1990; Pijn and Lopes Da Silva, 1993). This analytical method has recently been used by us to measure the degree and direction of functional coupling between neuronal populations (Wendling et al., 2001). The method is outlined in Appendix A. In brief, nonlinear regression analysis provides a parameter, referred to as the nonlinear correlation coefficient h^2, that takes its values in [0,1]. Low values of h^2 denote that signals X and Y are independent. On the contrary, high values of h^2 mean that signal Y may be explained by a transformation

Table 1
Patients data

Patients	Gender/ age	Historical findings	Type of epilepsy	MRI abnormalities	Number of recorded seizures	Patterns subtypes		Prominent electrophysiological subtype studied
						Type 1	Type 2	
BIG	F/43	FS at 8 months (encephalitis)	L-MTLE	Bilateral HS, left > right	2		2	2
BRE	F/31		R-MTLE	Normal	5	1	4	2
CAN	M/28	FS at 6 years	L-MTLE	Left HS	2	2		1
CLE	M/30		L-MTLE	Left HS	4	1	3	2
CRO	F/14	FS at	L-MTLE	Left HS	4	4		1
GAR	M/30	FS at 15 months	R-MTLE	Right HS, left frontal arachnoidian cyst	6	5	1	1
GON	F/31	FS at 2 years	L-MTLE	Left HS	1		1	1
GOS	F/30	Encephalitis at age 7	L-MTLE	Left HS	7		7	2
MAR	M/15		L-MTLE	Left HS	6	5	1	1
PAS	F/35	FS at 11 months	R-MTLE	Right HS	2	2		1
SCH	F/38	FS from 1 to 2 years, familial history epilepsy	L-MTLE	Bilateral HS, left > right	3	3		1
TAL	M/35		L-MTLE	Normal	2		2	2

Abbreviations: M: male, F: female, FS: febrile seizure; R-MTLE: right mesial temproal lobe epilepsy; L-MTLE: left mesial temproal lobe epilepsy, HS: MRI suggestive of hippocampal sclerosis (atrophy and hyperintensity on T2 sequences).

(possibly nonlinear) of signal X, i.e. signals X and Y are dependent. In addition to the estimation of h^2, a second quantity is evaluated that brings information on the causal property of the association. This quantity, referred to as the direction index D, takes into account both the estimated time delay τ between signals X and Y (latency) and the asymmetrical nature of the nonlinear correlation coefficient h^2 (values of the h^2 coefficient are different if the computation is performed from X to Y or from Y to X). Values of parameter D range from -1.0 (X is driven by Y) to 1.0 (Y is driven by X).

Signals were sampled at 256 Hz; this consideration leads to choose a length of 4 s for the analysis window sliding by steps of 0.25 s (Fig. 5a and c). h^2 values were averaged over each period of interest (BKG, BRD, DRD and ARD, defined above), for each pair of signal (HIP–AMY, HIP–EC and AMY–EC) and for each recording. The above parameter setting (4 s window with 0.25 s steps) leads to a number of 24 h^2 values averaged over a period of 10 s.

Results were represented in a graph that provides average values and standard deviations as a function of the considered period (Fig. 5d). In this representation, an arrow is used to indicate unidirectional coupling direction, when significant i.e. when two conditions are satisfied: i) h^2 value is significantly high (signals are correlated) and ii) $D \geq 0.5$ (asymmetry and time delay measures indicate the same direction of coupling, by a majority).

2.3. Statistical analysis

Statistical analysis focused on h^2 values, averaged over periods of interest in order to determine if significant differences exist in the evolution of correlation values computed between signals from hippocampus, amygdala and entorhinal cortex over the background (BKG), the pre-ictal (BRD) and the ictal (DRD and ARD) periods. For each patient and for each pair of signals, averaged h^2 values were first normalized according to the following equation $w = (1/2)\ln((1 + r)/(1 - r))$ in order to make their distribution Gaussian (Bendat and Piersol, 1971). Then, a student's t-test and a one-way analysis of variance were performed in order to determine whether normalized distributions of correlation values averaged over the BKG, BRD, DRD and ARD periods have the same or significantly different mean. A standard tool of numerical analysis (Matlab's ANOVA routine, statistics toolbox) was used.

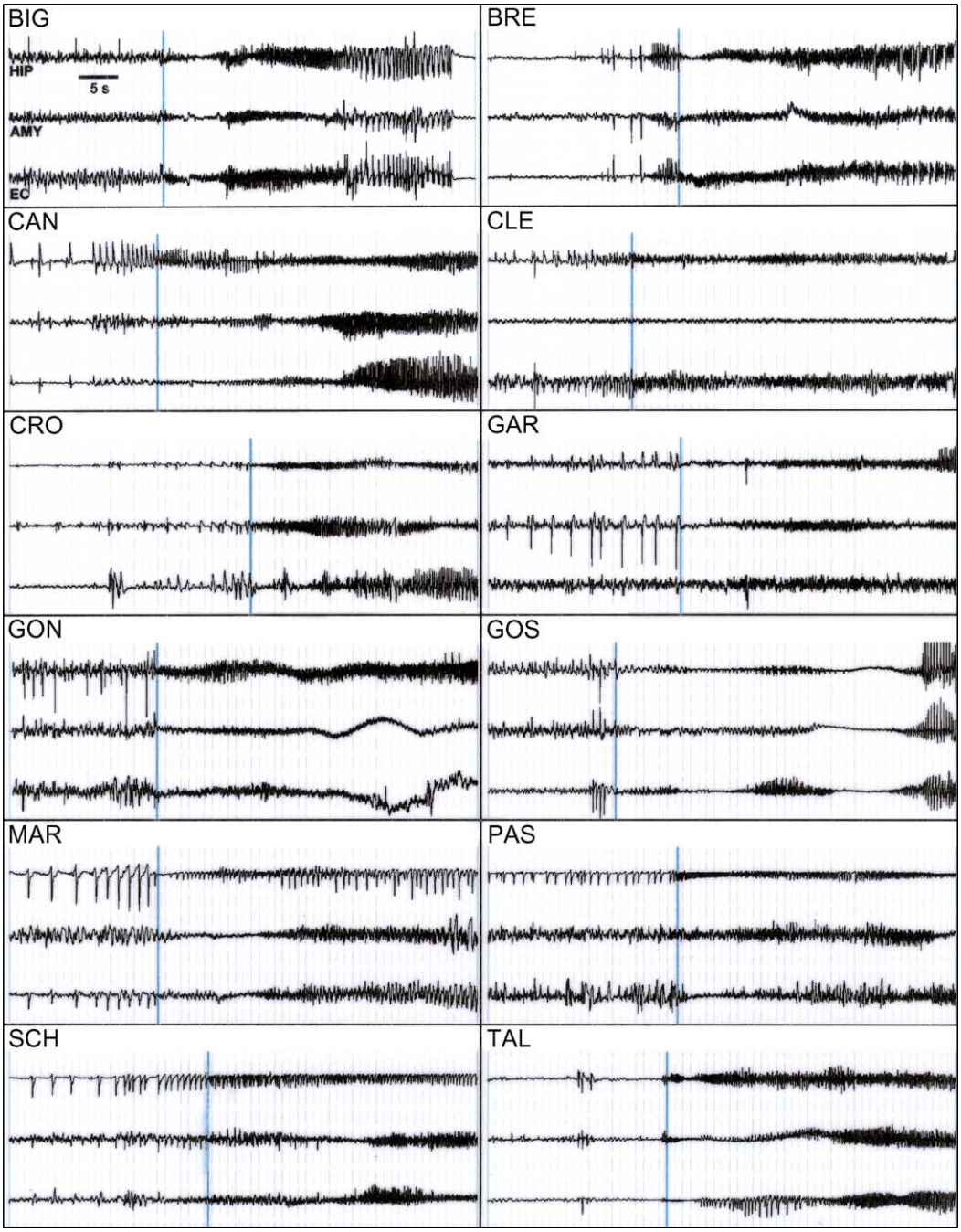

Fig. 2. Typical interictal to ictal transition electrophysiological patterns observed in the 12 studied patients. In each case, a 1 min period is displayed. Upper, middle and lower traces correspond to bipolar SEEG signals recorded from the hippocampus (HIP), amygdala (AMY) and entorhinal cortex (EC), respectively. The onset of the rapid discharge is marked by the vertical line. Pattern 1 was observed in patients CAN, CRO, GAR, MAR, PAS, SCH) and pattern 2 in patients BIG, BRE, CLE, GON, GOS, TAL.

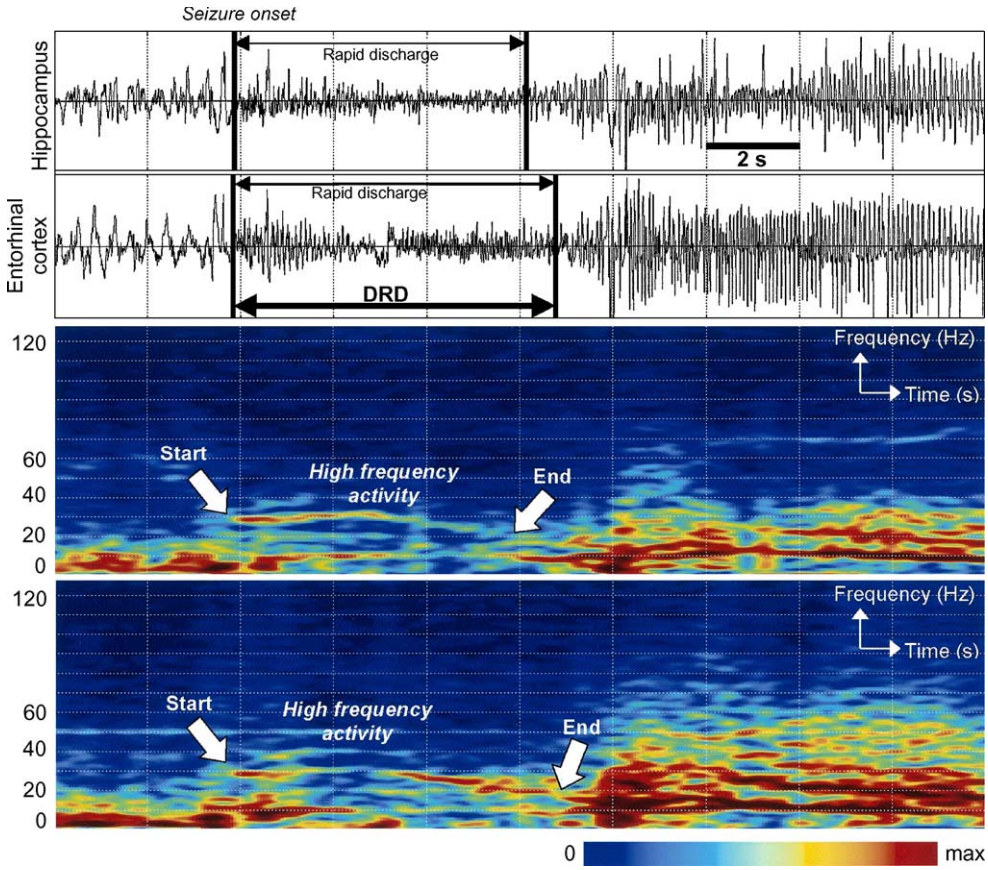

Fig. 3. Time–frequency representation (TFR) of SEEG signals recorded from the hippocampus and entorhinal cortex at seizure onset in patient BIG (energy distribution computed from the spectrogram obtained with short-term FFT computed over a 1 s duration sliding window). TFR is used to reveal the high-frequency activity (around 30 Hz, lower EEG gamma band) corresponding to the rapid discharge and to delimit this discharge in time. The DRD period ("During Rapid Discharge") is defined as the union of EEG segments exhibiting high-frequency activity at seizure onset.

3. Results

3.1. Visual inspection of SEEG signals and analysis of power spectral densities

All selected seizures started from the mesial region of the temporal lobe. Signals recorded by electrodes sampling other temporal lobe regions (i.e., neocortex, temporo-basal cortex, insular cortex) as well as from electrodes positioned in frontal and parietal lobe, did not show EEG modifications, indicating that these regions were not involved at seizure onset. All seizures were characterized by the appearance of a rapid discharge in the three considered mesial structures. The duration of rapid discharges (and thus the duration of the DRD period) was found to vary from patient to patient (8.9 ± 3.2 s, Table 2).

The transition between interictal period and ictal rapid discharges could be classified into two categories according to two main patterns defined in previous studies ((Engel et al., 1989; Spencer et al., 1992; Velasco et al., 2000a) (Fig. 2). In the first pattern ("type 1"), the transition from interictal to ictal activity was characterized by the emergence of a low-frequency, high-amplitude rhythmic spiking followed by the rapid discharge. In the second pattern ("type 2"), the seizure onset was characterized by the emergence of the rapid discharge without prior spiking. Eight patients (63%)

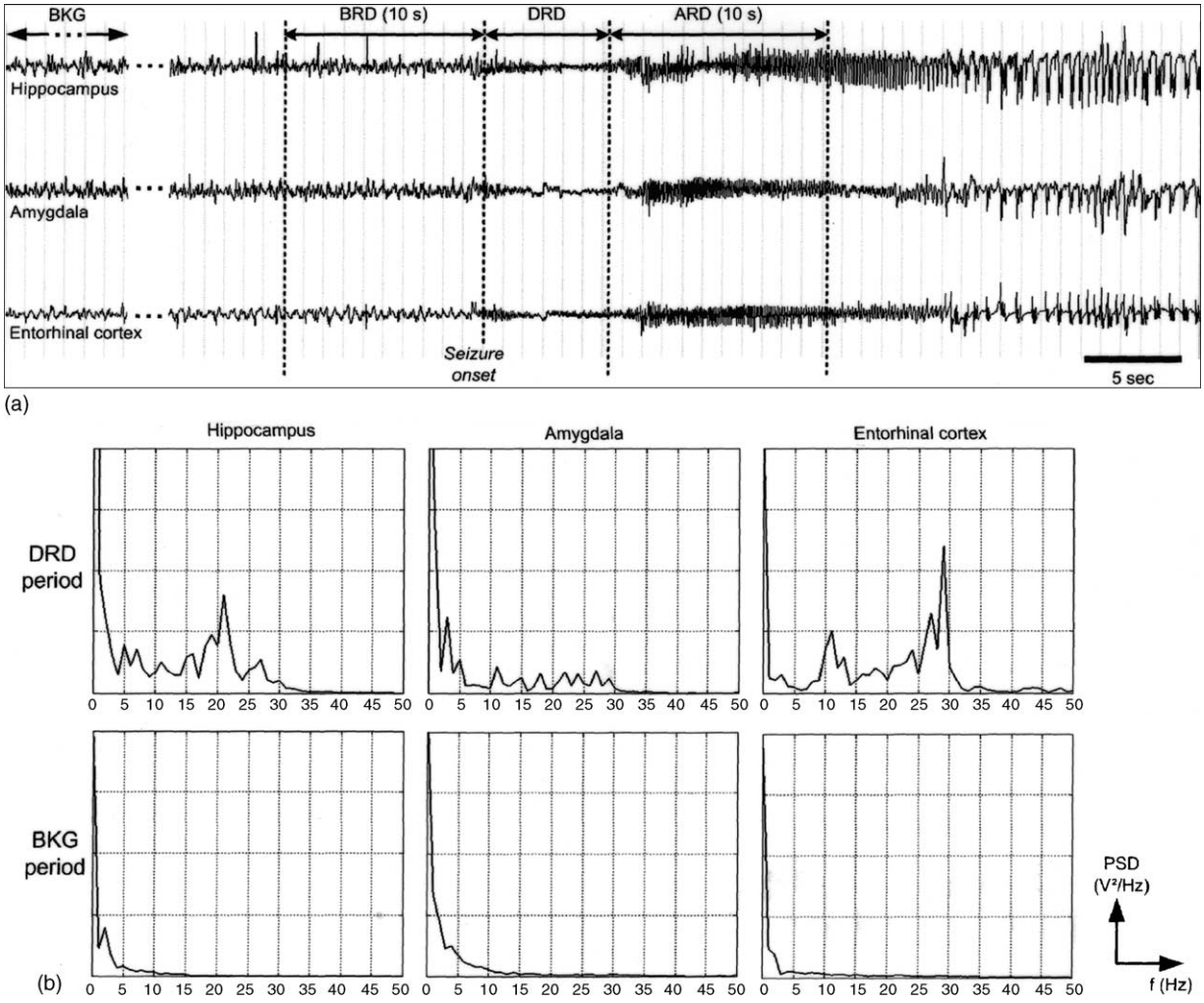

Fig. 4. (a) Delimitation of periods of interest. The first defined period corresponds to the rapid discharge that occurs at seizure onset (DRD period, visually defined, see Fig. 3). From the delimitation in time of the DRD period, two other periods (BRD and ARD) are defined. The BRD (respectively ARD) period corresponds to the 10 s interval that precedes (respectively follows) the DRD period. A fourth period of interest (BKG) that corresponds to background SEEG activity is also chosen for use as the reference period for quantitative comparison of spectral features and cross-correlations. (b) In each patient, the normalized power spectral density (PSD) of signals recorded from the hippocampus, amygdala and entorhinal over the DRD period was compared to that computed over the BKG period. It revealed the presence of fast oscillations (beta—12–24 Hz—and low gamma frequency bands−25–35 Hz) at seizure onset that are not present in signals recorded during background activity (BKG).

were found to have a single type of electrophysiological pattern at seizure onset (type 1: 4 patients; type 2: 4 patients) (Table 1). Four patients were found to have both types of seizure onset pattern. However, in these cases we found that one type was predominant.

Power spectral densities for each signal recorded from hippocampus, amygdala and entorhinal cortex confirmed visual inspection. A typical example is illustrated in Fig. 4(b). During the BKG period, signal energy was always distributed over low-frequency bands (i.e. up to 12 Hz). In contrast, during the DRD period, energy re-distributed over higher frequency bands, preferentially in beta and low gamma bands (from 12 to 35 Hz).

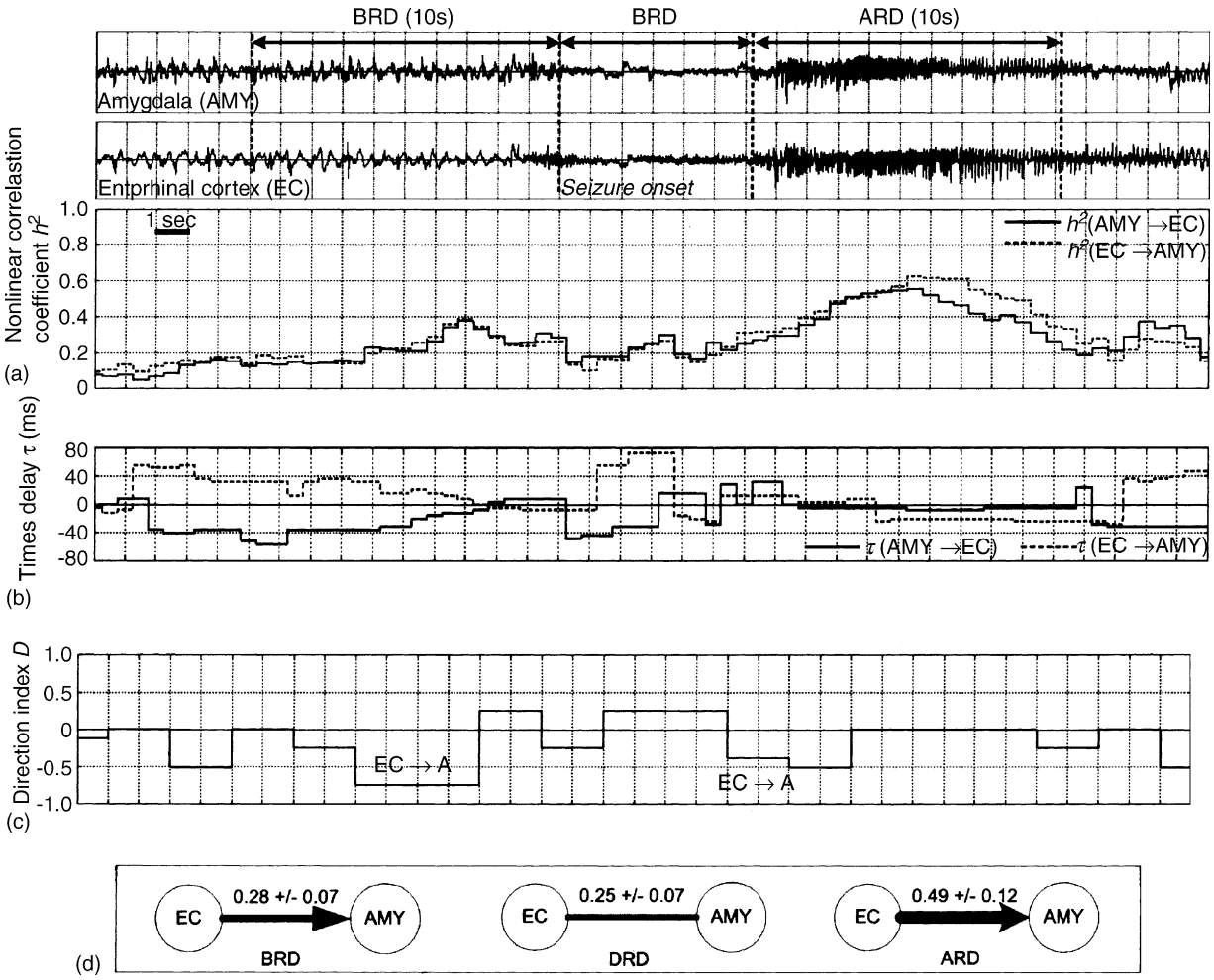

Fig. 5. Signal processing procedure used to characterize coupling between structures from signals they generate. On each pair of signals, nonlinear regression analysis is used to compute (a) the nonlinear correlation coefficient h^2 and (b) the time delay τ from upper signal to lower (solid line, AMY to EC) and vice-versa (dotted line, EC to AMY). (c) Asymmetry information (difference between h^2 coefficients) and time delays are jointly used to compute the direction index D that characterizes the direction of coupling. When greater than 0.5 (respectively lower than −0.5), D indicates a coupling from upper to lower signal (respectively lower to upper signal). (d) h^2 values are averaged over considered periods and information is represented as a graph in which line thickness is proportional to the average h^2 value and in which the arrow indicates coupling direction, when significant. Standard deviation of coefficient h^2 is also provided.

3.2. Cross-correlations of signals from mesial structures

Fig. 6 shows graphs providing the average value and standard deviation of nonlinear correlation coefficient h^2 computed over each period of interest and for each pair of signals (HIP–AMY, HIP–EC and AMY–EC). The BRD period was characterized by significant values indicating strong interactions between mesial temporal structures compared to the BKG period. Interactions between HIP and EC were predominant, observed in 10/12 cases (83%). Interactions between EC and AMY were observed in 6/12 cases (50%) and between AMY and HIP in 7/12 cases (58%). The analysis of coupling directionality characterized by the direction index D indicated that most of the couplings were driven either by HIP (in six patients) or by the EC (in four patients). Only one patient had interaction

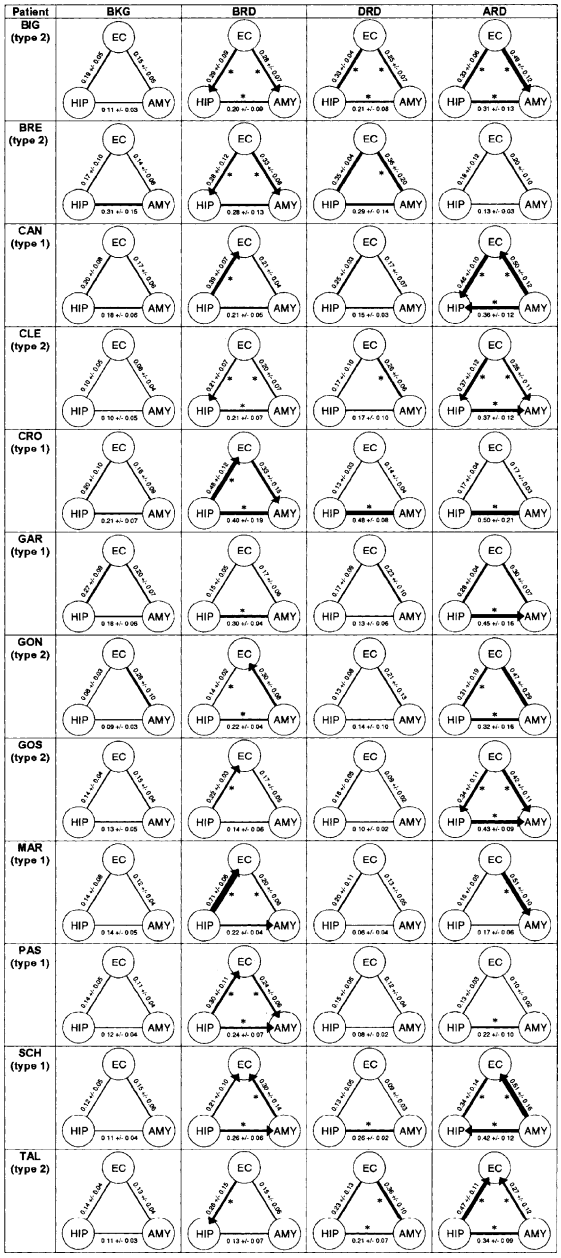

Fig. 6. Results obtained in the 12 studied patients. For each period (BKG, BRD, DRD, and ARD) and for each triplet of signals (recorded from HIP, AMY and EC), average h^2 values and standard deviations as well as D values are represented as a graph. Thicker lines indicate higher correlations. Arrows indicate coupling direction. Asterisk indicates significantly high values (+ 2 standard deviations) with respect to those computed over the BKG period.

Table 2
Duration of the rapid discharge period (DRD) and electrophysiological subtype of interictal to ictal transition (types 1 or 2)

Patients	DRD period duration (s)	Type
BIG	6.3	2
BRE	6.5	2
CAN	9.1	1
CLE	15.3	2
CRO	4.4	1
GAR	11.3	1
GON	9.3	2
GOS	9.2	2
MAR	12.9	1
PAS	6.7	1
SCH	10.3	1
TAL	5.5	2

in which the amygdala seemed to play the leader role (Fig. 6).

The DRD period was characterized by a decrease in h^2 values indicating a drop of the degree of coupling between considered structures for most combinations, while the ARD period disclosed a marked re-increase of values denoting a new strengthening of couplings after the rapid discharge. This result was confirmed by analyzing the estimated average h^2 values. Statistical results are presented in Fig. 7 that shows normalized h^2 values (cf. Section 2.3). The empirical distribution of normalized h^2 values, displayed in Fig. 7(b), are assumed to be Gaussian. A conventional t-test was then performed to measure the significance of observed differences of mean (Fig. 7, legend). As shown in Fig. 7(b), the correlation values measured during the BRD period are statistically higher than those measured during the BKG periods. Values obtained in DRD period were significantly lower than the values obtained during the BRD and the ARD periods. Results displayed in Fig. 7(c) in the form of a so-called "boxplot", confirmed those obtained with the t-test. The lower and upper lines of each "box" (25th and 75th percentiles of each sample) and the line in the middle of the box (sample median), respectively, indicates that the distribution of normalized h^2 values during the BRD period are significantly higher than values measured over the BKG and DRD periods.

Finally, one can also notice the presence of five outliers in the boxplot of Fig. 7(c) (symbol "+") that do not contradict the above results. Indeed, in two patients h^2 values (HIP–EC) measured over the BRD period

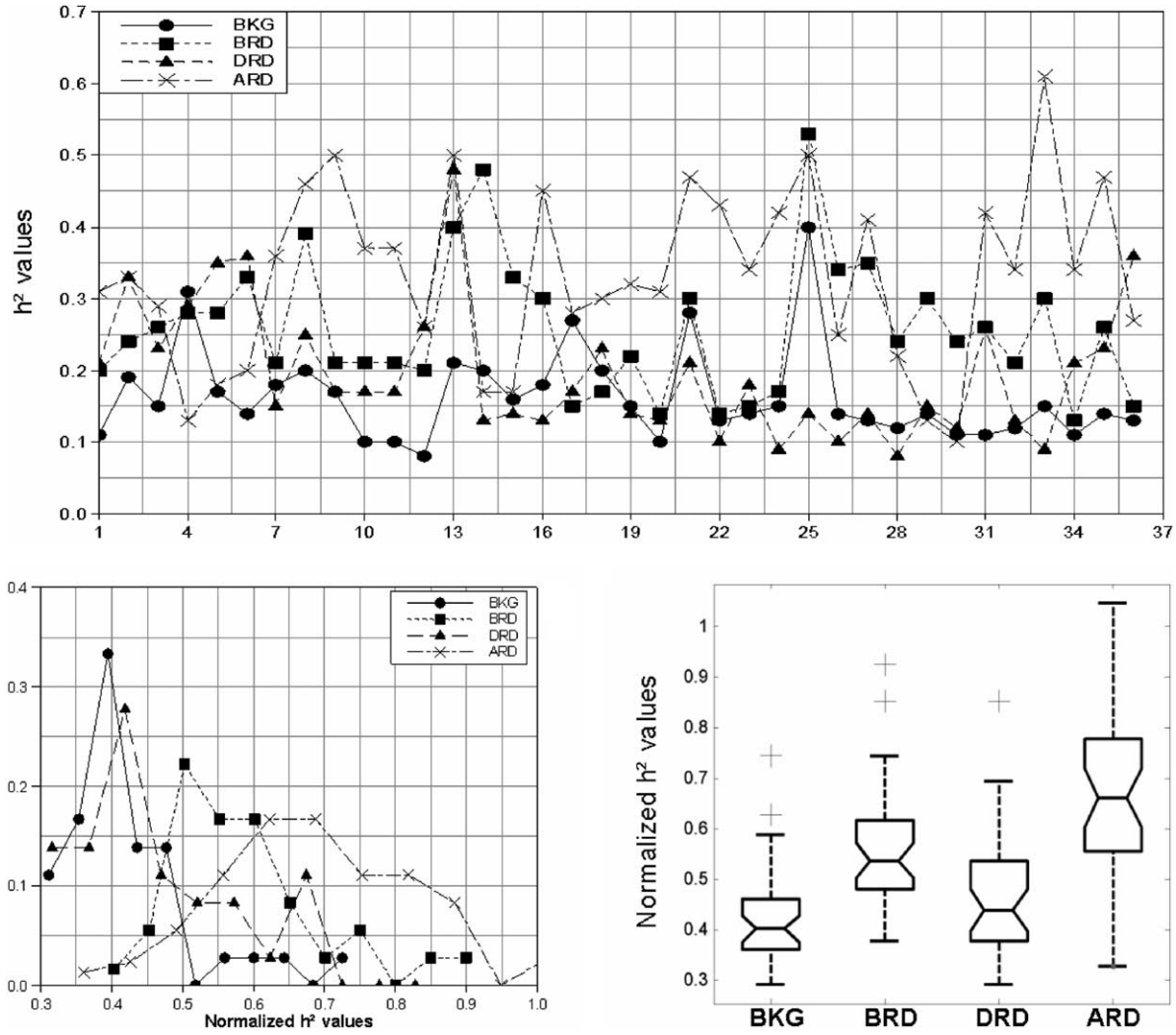

Fig. 7. Results of statistical analysis performed to test the significance of the observed differences between correlation values measured over considered periods. (a) The 36 average h^2 values (3 pairs of signals per patient, 12 patients) are first normalized in order to make their distribution as Gaussian (b) before performing statistical tests. (c) Boxplot performed on normalized values. The lower and upper lines of each "box" (25th and 75th percentiles of each sample) and the line in the middle of the box (sample median), respectively, indicate that the distributions of h^2 values over the BKG, BRD and DRD periods are narrower than that computed over the ARD period. The "whiskers" (lines extending above and below the box) show the extent of the rest of the sample. The notches in boxes graphically show the confidence interval (95%) about the median of each distribution. The fact that they do not intersect indicates that means significantly differ from period to period: h^2 values measured before the rapid discharge (BRD) are significantly higher than those measured during background activity (BKG) and during the rapid discharge itself (DRD). For the period that follows the rapid discharge (ARD) strong re-coupling is indicated by significantly high h^2 values. See text for information about outliers (plus signs). Student's *t*-test indicate significantly different means of h^2 values between BKG and BRD periods (P = 1.8E−06), BRD and DRD periods (P = 2.7E−03) and DRD and ARD periods (P = 7.0E−07).

were found to be higher than the mean of h^2 values computed in all patients. This indicates a stronger preictal synchrony. In two other patients the same observation could be obtained by analyzing the BKG period (HIP–AMY and HIP–EC, respectively). Finally, the fifth outlier corresponds to the only h^2 value measured on the DRD period that deviates from the distribution of values over this period (higher than the mean).

3.3. Relationship between correlation values and interictal/ictal transition patterns

We also investigated whether the interactions between limbic structures differed as a function of the two visually defined patterns (type 1 and type 2) observed during transition from interictal to ictal activity. Fig. 8(a) shows the number of significant coupling values obtained in the two pattern-based groups during the BRD period. Type 1 was characterized by interactions that uniformly involve the three structures. Interestingly, in the type 2 group, interactions seemed to predominate between EC and HIP. Finally, by analyzing the direction index during the BRD period, we found that the HIP was always the leader structure in the type 1 seizure pattern whereas in the type 2 seizure pattern, EC was the leader structure in the majority of cases (Fig. 8b).

4. Discussion

This study demonstrates that SEEG signals recorded from limbic structures of the temporal lobe are characterized by a significantly high correlation during the period preceding the appearance of rapid epileptic discharges. This first period of "synchrony" was also followed by a period of "desynchrony", that corresponds to the appearance of rapid discharges, marked by a

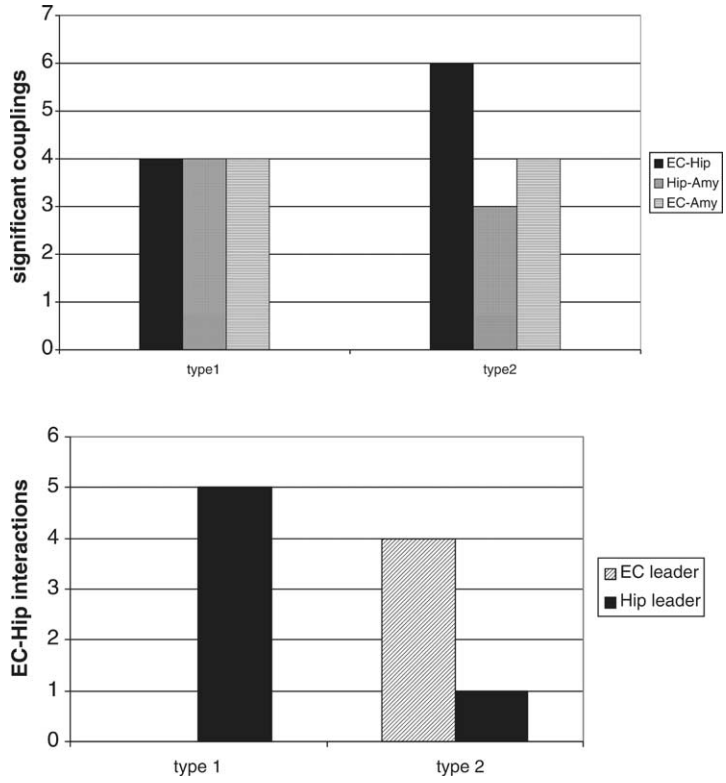

Fig. 8. (a) Number of significant interactions determined by nonlinear regression analysis (h^2) during the BRD period between amygdala (Amy), hippocampus (Hip) and entorhinal cortex (EC) in type 1 and type 2 seizures. (b) This graph shows the proportion of EC-Hip interactions in which the EC or the Hip is leader according to the seizure subtype.

decrease of cross-correlation. To our knowledge this result has not been shown previously and warrants discussion from several points of view.

Firstly, we have characterized the interactions between different limbic areas by computing the cross-correlation of SEEG signals. In previous decades numerous methods for computation of synchronization between EEG signals have been proposed, both linear (such as coherence analysis), and nonlinear (such as mutual information); these have been used not only in the field of epilepsy but also in cognitive science. Although results may differ from one method to the other several recent studies have tended to show that, qualitatively, results are similar (Quian Quiroga et al., 2002). In the past, we mainly used a nonlinear method based on nonlinear regression analysis, whose first application to EEG signals was proposed by the Amsterdam group (Lopes da Silva et al., 1989; Pijn and Lopes Da Silva, 1993). This method is known to give a robust estimate of the statistical coupling between two signals (coefficient h^2). Recently, we have complemented this by adding an estimate of the direction of coupling (Wendling et al., 2001).

Using these two indices (coefficient h^2 and direction index), we characterized the functional coupling between mesial structures at seizure onset and over the periods that immediately precede and follow seizure onset (i.e. transition from interictal to ictal activity), and compared results with those obtained over a reference period of background activity. In this sense, our study differs from recent work dealing with the detection of EEG changes several minutes or even hours before the occurrence of seizure discharges (Le Van Quyen et al., 2001; Mormann et al., 2003). Some of these studies suggest that a pre-ictal decrease in synchrony, lasting for several minutes or hours, is a predisposing factor for seizure development. Our results are not in disagreement with these studies, since the increase in synchrony we observed takes place just a few seconds before the emergence of the rapid ictal discharge.

Secondly, the rapid ictal discharge always involved distant and functionally distinct mesial temporal structures (HIP, AMY and EC) almost simultaneously. In a previous report we hypothesized the existence of a "synchronizing system" that would provide to the simultaneous onset of fast activity (Wendling et al., 2003). The present study confirms this hypothesis, demonstrating that pre-ictal synchronization between mesial structures is the initial event for seizures starting in the mesial temporal region. Detailed analysis of correlation and direction indices values showed that the hippocampus was involved in most of the significant couplings, and that the entorhinal cortex could be the leading structure in some situations. We have also found that the amygdala is more rarely involved. These results give strength to the hypothesis of a hyperexcitable limbic network in which the "driving input" may arise from one of the mesial structures. In addition, recent studies have shown that subiculum could also be an important site of epileptic activity (Cohen et al., 2002). The implantation of electrodes in our patients did not allow us to specifically explore this part of the hippocampal region. We therefore cannot exclude the possible participation of this structure in the network synchronisation observed at seizure onset.

Two different electrophysiological patterns of pre-ictal synchrony were observed during the interictal to ictal transition period. The first one (emergence of a low-frequency, high-amplitude rhythmic spiking followed by a tonic discharge (Spencer et al., 1992; Velasco et al., 2000a)) was characterized by an initial synchronization between the three mesial structures. For this first pattern, our data suggests that spiking activity is more likely to be triggered by the hippocampus than by the EC. This result is in agreement with the interpretation of Spencer and Spencer (1994) who also suggested that pre-ictal spiking was not related to EC activity but rather was of hippocampal origin. We also found that the EC was constantly involved during the tonic phase and we interpret its role as a propagation route to other structures, in particular the neocortex. Indeed, numerous direct reciprocal connections exist between these two structures, while the connections between hippocampus and neocortex are mainly indirect passing through the EC (Amaral and Insausti, 1990).

In the second pattern, the scenario was found to be different. The evident synchrony over the BRD period took place in the absence of pre-ictal spiking. The BRD period interactions were predominately between HIP and EC, and in this case the EC was found to be the driving source of this synchrony. This result suggests that synchronized oscillations take place before the emergence of the rapid discharge and are initiated in the EC.

Numerous experimental works have demonstrated that the EC could be a key structure in the genesis of ictal activity in vitro. Most of these experiments were performed using combined slices of rat hippocampus-entorhinal cortex treated with chemical convulsants. In this type of preparation, prolonged ictal discharges are initiated in the deep layers of the entorhinal cortex and propagate to the hippocampus proper via the perforant path/dentate gyrus (Barbarosie and Avoli, 1997; Heinemann et al., 1993; Jones et al., 1992). Under these conditions, the EC is prone to display sustained tonic ictal discharges, more prolonged than those occurring in the hippocampus (Heinemann et al., 1993). Because of its intrinsic properties and connectivity it has been proposed that the EC is essential to amplify and sustain temporal lobe seizures (Bear and Lothman, 1993). Interestingly, in a chronic in vivo model of epilepsy (unilateral intrahippocampal injections of kainic acid (KA) in rats), low-voltage fast activity (similar to human pattern 2) and hypersynchronous (similar to pattern 1) electrographic ictal-onset patterns were observed (Bragin et al., 1999). As in human tissue, hypersynchronous ictal-onsets originated predominantly in hippocampus, whereas low-voltage fast ictal-onsets more often involved extrahippocampal structures.

Finally, our findings suggest that, after the structures are initially synchronized (BRD period), spatial correlation then significantly decreases during the period of rapid discharge suggesting an uncoupling of brain sites involved in fast oscillations. These results are in line with those previously reported by us (Wendling et al., 2003), namely, that very fast oscillations (> 60 Hz) in frontal lobe seizures are decorrelated even if the frequency bands of signals recorded in mesial temporal structures in the present study are lower (beta and low gamma) than those recorded in frontal neocortical structures.

In summary, these results provide evidence supporting the existence of strong interactions between limbic networks at seizure onset. These interactions take place during the period preceding the appearance of rapid discharge and may represent a pre-requisite condition for initiation of ictal activity. The respective roles of the entorhinal cortex and the hippocampus are reflected by the electrophysiological pattern of the inter-ictal to ictal transition period. These results show that the organization of the epileptogenic zone in MTLE cannot readily be reduced to a single “focus” and that a more complex network configuration is probably responsible for the initiation of seizure activity. From a therapeutic perspective, the detection of pre-ictal synchrony between mesial structures could offer a means of reliably detecting modifications preceding seizures and thus potentially allowing depth chronic stimulations, a promising method in the treatment of MTLE (Velasco et al., 2000b; Vonck et al., 2002). In addition, the precise identification of the epileptogenic networks involved in limbic seizures in human MTLE could facilitate more tailored surgical approaches (Regis et al., 2000).

Acknowledgements

The authors wish to thank Professor Massimo Avoli for his constructive suggestions and valuable comments on the present work and Dr Aileen McGonigal for the revision of the English version of this paper and for helpful comments.

Appendix A

Nonlinear regression analysis provides an estimate of the degree of association between two signals X and Y independently from the linear or nonlinear nature of this association. The basic idea is to describe the amplitude of signal Y as a function of the amplitude of signal X using a nonlinear regression curve and to compute the variance of Y that is explained, or predicted, by X according to this regression curve. In practice, a parameter referred to as the nonlinear correlation coefficient h^2, which takes its values in [0,1], is computed. Low values of h^2 denote that signals X and Y are independent. On the opposite, high values of h^2 mean that signal Y may be explained by a transformation (possibly nonlinear) of signal X, i.e. signals X and Y are dependent. In addition to the estimation of h^2, a second quantity referred to as the direction index D, is computed based on both the estimated time delay τ between signals X and Y (latency), and the asymmetrical nature of the nonlinear correlation coefficient h^2. Values of parameter D range from -1.0 (X is driven by Y) to 1.0 (Y is driven by X). In order to follow the temporal evolution of the correlation between signals X and Y, estimation of coefficient h^2 and direction index D is performed over a

temporal sliding window of fixed duration. Statistical properties of estimated quantities h^2 and D (bias, variance) were also studied in previous studies (Wendling et al., 2001) and performances were evaluated in real situations (temporal lobe epilepsy (Bartolomei et al., 2001)). According to these studies, reliable estimation of parameters h^2 and D is obtained for scatterplots (Y versus X) that include one thousand points, at least.

References

Amaral, D., Insausti, R., 1990. Hippocampal formation. In: Paxinos, G. (Ed.), The Human Nervous System. Academic Press, San Diego, pp. 711–757.

Avoli, M., D'Antuono, M., Louvel, J., Kohling, R., Biagini, G., Pumain, R., D'Arcangelo, G., Tancredi, V., 2002. Network and pharmacological mechanisms leading to epileptiform synchronization in the limbic system in vitro. Prog. Neurobiol. 68, 167–207.

Bancaud, J., 1981. Epileptic attacks of temporal lobe origin in man. Jpn. J. EEG EMG, Suppl. Didactic Lectures, Xth ICECN, Kyoto, 61–71.

Barbarosie, M., Avoli, M., 1997. CA3 driven hippocampal entorhinal loop controls raher that sustains in vitro limbic seizures. J. Neurosci. 17, 9308–9314.

Barbarosie, M., Louvel, J., Kurcewicz, I., Avoli, M., 2000. CA3-Released entorhinal seizures disclose dentate gyrus epileptogenicity and unmask a temporoammonic pathway. J. Neurophysiol. 83, 1115–1124.

Bartolomei, F., Wendling, F., Bellanger, J., Regis, J., Chauvel, P., 2001. Neural networks involved in temporal lobe seizures: a nonlinear regression analysis of SEEG signals interdependencies. Clin. Neurophysiol. 112, 1746–1760.

Bear, J., Lothman, E.W., 1993. An in vitro study of focal epileptogenesis in combined hippocampal-parahippocampal slices. Epilepsy Res. 14, 183–193.

Bendat, J., Piersol, A., 1971. Random Data: Analysis and Measurement Procedures. Wiley-Interscience.

Bernasconi, N., Bernasconi, A., Andermann, F., Dubeau, F., Feindel, W., Reutens, D.C., 1999. Entorhinal cortex in temporal lobe epilepsy: a quantitative MRI study. Neurology 52, 1870–1876.

Bernasconi, N., Bernasconi, A., Caramanos, Z., Andermann, F., Dubeau, F., Arnold, D.L., 2000. Morphometric MRI analysis of the parahippocampal region in temporal lobe epilepsy. Ann. N. Y. Acad. Sci. 911, 495–500.

Bertram, E.H., Zhang, D.X., Mangan, P., Fountain, N., Rempe, D., 1998. Functional anatomy of limbic epilepsy: a proposal for central synchronization of a diffusely hyperexcitable network. Epilepsy Res. 32, 194–205.

Bragin, A., Engel Jr., J., Wilson, C.L., Fried, I., Mathern, G.W., 1999. Hippocampal and entorhinal cortex high-frequency oscillations (100–500 Hz) in human epileptic brain and in kainic acid-treated rats with chronic seizures. Epilepsia 40, 127–137.

Cohen, I., Navarro, V., Clemenceau, S., Baulac, M., Miles, R., 2002. On the origin of interictal activity in human temporal lobe epilepsy in vitro. Science 298, 1418–1421.

Du, F., Whetsell, W., Abou-Khalil, B., Blumenkopf, B., Lothman, E., Schwarcz, R., 1993. Preferential neuronal loss in layer III of the entorhinal cortex in patients with temporal lobe epilepsy. Epilepsy Res. 16, 223–233.

Engel Jr., J., Babb, T.L., Crandall, P.H., 1989. Surgical treatment of epilepsy: opportunities for research into basic mechanisms of human brain function. Acta. Neurochir. Suppl. (Wien) 46, 3–8.

Heinemann, U., Zhang, C.L., Eder, C., 1993. Entorhinal cortex-hippocampal interactions in normal and epileptic temporal lobe. Hippocampus 3, Spec No. (89-97).

Insausti, R., Tunon, T., Sobreviela, T., Insausti, A., Gonzalo, L., 1995. The human entorhinal cortex: a cytoarchitectonic analysis. J. Comp. Neurol. 355, 171–198.

Jones, R., Heinemann, U., Lambert, J., 1992. The entorhinal cortex and generation of seizure activity: studies of normal synaptic transmission and epileptogenesis in vitro. In: Avanzini, G., Engel, J., Fariello, R., Heinemann, U. (Eds.), Neurotransmitters in Epilepsy. Elsevier Science, pp. 173–180.

Jutila, L., Ylinen, A., Partanen, K., Alafuzoff, I., Mervaala, E., Partanen, J., Vapalahti, M., Vainio, P., Pitkanen, A., 2001. MR volumetry of the entorhinal, perirhinal, and temporopolar cortices in drug-refractory temporal lobe epilepsy. AJNR Am. J. Neuroradiol. 22, 1490–1501.

King, D., Spencer, S., McCarthy, G., Spencer, D., 1997. Surface and depth EEG findings in patients with hippocampal atrophy. Neurology 48, 1363–1367.

Le Van Quyen, M., Martinerie, J., Navarro, V., Baulac, Varela, F.J., 2001. Characterizing neurodynamic changes before seizures. J. Clin. Neurophysiol. 18, 191–208.

Lopes da Silva, F., Pijn, J.P., Boeijinga, P., 1989. Interdependence of EEG signals: linear vs. nonlinear associations and the significance of time delays and phase shifts. Brain Topogr. 2, 9–18.

Lothman, E., Bertram, I., Stringer, J., 1991. Functional anatomy of hippocampal seizures. Prog. Neurobiol. 37, 1–82.

Meeren, H.K., Pijn, J.P., Van Luijtelaar, E.L., Coenen, A.M., Lopes da Silva, F.H., 2002. Cortical focus drives widespread corticothalamic networks during spontaneous absence seizures in rats. J. Neurosci. 22, 1480–1495.

Mormann, F., Kreuz, T., Andrzejak, R.G., David, P., Lehnertz, K., Elger, C.E., 2003. Epileptic seizures are preceded by a decrease in synchronization. Epilepsy Res. 53, 173–185.

Musolino, A., Tournoux, P., Missir, O., Talairach, J., 1990. Methodology of in vivo anatomical study and stereo-electroencephalographic exploration in brain surgery for epilepsy. J. Neuroradiol. 17, 67–102.

Pijn, J., 1990. Quantitative evaluation of EEG signals in epilepsy, nonlinear associations,time delays and nonlinear dynamics. PhD Thesis. University of Amsterdam, Amsterdam.

Pijn, J., Lopes Da Silva, F., 1993. Propagation of electrical activity: nonlinear associations and time delays between EEG signals. In: Zschocke, Speckmann (Eds.), Basic Mechanisms of the EEG. Birkauser, Boston.

Quian Quiroga, R., Kraskov, A., Kreuz, T., Grassberger, P., 2002. Performance of different synchronization measures in real data:

a case study on electroencephalographic signals. Phys. Rev. E Stat. Nonlin. Soft Matter Phys. 65, 041903.

Regis, J., Bartolomei, F., Rey, M., Hayashi, M., Chauvel, P., Peragut, J., 2000. Gamma knife surgery for mesial temporal lobe epilepsy. J. Neurosurg. 93 (Suppl. 3), 141–146.

Spencer, S., Guimaraes, P., Katz, A., Kim, J., Spencer, D., 1992. Morphological patterns of seizures recorded intracranially. Epilepsia 33, 537–545.

Spencer, S., Spencer, D., 1994. Entorhinal-hippocampal interactions in medial temporal lobe epilepsy. Epilepsia 35, 721–727.

Talairach, J., Bancaud, J., Szickla, G., Bonis, A., Geier, S., 1974. Approche nouvelle de la chirurgie de l'épilepsie: methodologie stéréotaxique et résultats thérapeutiques. Neurochirurgie 20 (Suppl. 1), 1–240.

Velasco, A., Wilson, C., Babb, T., Engel, J., Functional, 2000a. Anatomic correlates of two frequently observed temporal lobe seizure onset patterns. Neural. Plast. 7, 49–63.

Velasco, A.L., Velasco, M., Velasco, F., Menes, D., Gordon, F., Rocha, L., Briones, M., Marquez, I., 2000b. Subacute and chronic electrical stimulation of the hippocampus on intractable temporal lobe seizures: preliminary report. Arch. Med. Res. 31, 316–328.

Vonck, K., Boon, P., Achten, E., De Reuck, J., Caemaert, J., 2002. Long-term amygdalohippocampal stimulation for refractory temporal lobe epilepsy. Ann. Neurol. 52, 556–565.

Wendling, F., Bartolomei, F., Bellanger, J., Chauvel, P., 2001. Interpretation of interdependencies in epileptic signals using a macroscopic physiological model of EEG. Clin. Neurophysiol. 112, 1201–1218.

Wendling, F., Bartolomei, F., Bellanger, J.J., Bourien, J., Chauvel, P., 2003. Epileptic fast intracerebral EEG activity: evidence for spatial decorrelation at seizure onset. Brain 126, 1449–1459.

Williamson, P., Engel, P., Munari, C., 1998. Anatomic classification of localization-related epilepsies. In: Engel, J., Pedley, T. (Eds.), Epilepsy: A Comprehensive Textbook. Lippincott-Raven, New York.